GROUND2023
&
10th LPE

International Conference on Grounding
&
Lightning Physics and Effects

Belo Horizonte, Brazil - May, 2023

THE LIGHTNING ATTACHMENT PROCESSES OBSERVED ON A SUBMICROSECOND-SCALE: MEASUREMENTS OF CURRENT AND VIDEO

Mathieu N. Plaisir[1], Amitabh Nag[1, 2], Kenneth L. Cummins[1, 3], Dylan J. Goldberg[1], Christopher J. Biagi[4], Robert G. Brown[4, 5], and Hamid K. Rassoul[1]
1. Florida Institute of Technology, 2. Los Alamos National Laboratory, 3. University of Arizona, 4. NASA Kennedy Space Center, and 5. University of Central Florida

Abstract - We examined current waveforms measured on the Kennedy Space Center (KSC) Industrial Area Tower (IAT) time-correlated with ultra-high-speed video camera records and broadband field measurements of two negative cloud-to-ground strokes that attached to the tower in June 2022. For the two strokes examined in this study, the measured return stroke peak currents were -30.5 kA and -34.5 kA. The attachment points between the upward and downward leaders were 78 and 72 m above our Franklin rod (175.7 and 169.7 m above ground level), respectively. Our observations confirm that the slow front in current begins during (toward the end of) the upward connecting leader (UCL) phase of a stroke and a rapid increase in the slow-front current occurs with the formation of the common streamer zone (CSZ). The attachment process is completed after the UCL and DL propagate within the CSZ and merge with each other, marking the onset of the fast transition in the current waveform. Thus, the "return stroke proper" starts with the fast transition in current and is preceded by the UCL and CSZ phases of the stroke.

1 – INTRODUCTION

The attachment of the downward negative leader with the upward positive connecting leader in negative cloud-to-ground lightning has been challenging to study due to the processes occurring on a sub-microsecond timescale (e.g., Saba et al., 2022; Plaisir et al., 2022; Jiang et al., 2021; Qi et al., 2019; Tran and Rakov, 2017, Khounate et al., 2021 [1-6]). Additionally, simultaneous optical, broadband electromagnetic fields, and current measurements of the attachment process in downward natural lightning are extremely rare and such observations are needed to decipher the details of the processes occurring during upward-to-downward leader attachment and the relationship between current and remotely measured fields during attachment.

The Industrial Area Tower (IAT) (Nag et al., 2021 [7]) at the Kennedy Space Center (KSC) is located in a region with flat ground experiencing lightning flash density in the range of 8 to 12 flashes/sq. km/year. A lightning current measurement system was installed on this 91.5 m tall tower supported by grounded guy wires and became operational on August 1, 2018. This relatively low-height (low enhancement) tower was selected in order to observe lightning attachment that exhibits the characteristics of natural lightning including short upward connecting and unconnected leaders in response to nearby downward leaders, natural first stroke onsets with slow-front and fast-transition characteristics, and natural first-stroke current waveforms. This is the only natural-lightning current measurement facility in the United States at present. We also installed an ultra-high-speed (up to 1,000,000 frames per second) video camera and broadband field measurements near the tower.

Two negative cloud-to-ground strokes attached to the tower in June 2022. In this study, we will focus on the lightning attachment processes for these strokes by examining correlated channel-base current waveforms and ultra-high-speed video camera records.

2 – MEASUREMENT SYSTEM AND DATA

The multi-channel current measurement system had a nominal measurement range of about 0.83 A to 350 kA, allowing the analysis of currents during both the upward leader and return-stroke stages. Characteristics of the four current-measurement channels at the IAT are shown in Table 1. The current waveforms were digitized with a 50 MHz sampling rate. A Phantom V2512 camera was located 752 m from the tower and was operated at 783k fps. The exposure time for each frame was 740 ns with 540 ns of dead time between frames. The camera and current measurement systems were independently GPS-timestamped. Broadband electromagnetic field measurement systems were located at a distance of 1.4 km from the tower, but those measurements are not analyzed in this paper.

Table 1 - Characteristics of the four current-measurement channels at the KSC IAT.

Current Measurement Device	Frequency Bandwidth	Current Saturation	RMS Noise Floor with Full Bandwidth	RMS Noise Floor with 1 MHz Bandwidth
Shunt	DC – 10 MHz	±900 A	0.83 A	0.41 A
		±24 kA	26.1 A	11.7 A
		±350 kA	80.7 A	38.8 A
Rogowski coil	0.05 Hz – 10 MHz	±200 kA	220 A	120 A

Two negative first strokes attached to the tower on June 6 and June 18, 2022 (strokes 060622 and 061822, respectively). Their measured return stroke peak currents were -30.5 kA and -34.5 kA, respectively. The peak currents reported by the U. S. National Lightning Detection Network (NLDN) for the two strokes were -23.3 and -28.8 kA, respectively. The tip of our Franklin rod was 97.7 m above ground level (AGL). The attachment points between the upward and downward leaders for the two strokes were 78 and 72 m above our Franklin rod (175.7 and 169.7 m AGL), respectively.

3 – ANALYSIS AND RESULTS

3.1 – STROKE 060622

Figure 1 shows six consecutive video camera frames recorded for stroke 060622. Each frame is an integration of light over 740 ns of exposure time and is followed by a 540 ns dead time (so the interframe interval was 1.28 μs). The field-of-view (FOV) of the camera extended from 77.1 to 269.6 m AGL. The top of the Franklin rod on our tower is indicated by the dashed line at 97.7 m AGL. We have labelled, as t ≡ 0, the first frame in which we observed the upward connecting leader (UCL) and the downward leader (DL) attached to each other. The common streamer zone (CSZ) was first observed two frames prior (t = -2.56 μs) to the attachment frame and had a length 16.1 m at that time. We show the zoomed-in view of the CSZ in the box below the frame. After the CSZ was formed, the UCL and DL propagated within the CSZ and in the frame immediately preceding the attachment frame, the gap between the UCL and DL was 8.5 m. In the frame following the attachment (t = 1.28 μs), the brightness of return stroke in progress nearly saturated the entire frame.

In order to time-align our video camera frames and current waveforms with accuracy better than the microsecond-scale uncertainty associated with the GPS-time-stamping system of our current measurement, we calculated the mean gray level of 9 pixels just above our Franklin rod in each camera-frame. We then plotted the inverted mean gray level along with the current waveform of our 900-A channel. We then time-aligned the rising edges of the luminosity and current pulses associated with the UCL. Such time-alignment between luminosity and current from spatially proximate locations provided us with alignment accuracy of hundreds of nanoseconds. The well-aligned data are seen in Figure 2. Using this time-alignment, we then overlaid in Figure 3 the exposure times of our video camera frames (indicated by pink rectangles) on top of the current waveform (shown on a 30-μs time window) measured by our 350-kA channel. The corresponding times for the video camera frames are indicated above and below each rectangle. The black vertical dashed line indicates the mid-point of the exposure time of the attachment frame (t ≡ 0). This frame occurred at the end of the slow front and the beginning of the fast transition. Additionally, we see that the frame (t = -2.56 μs) in which the CSZ is observed for the first time aligned with the portion of the slow front waveform where the current increased rapidly from the early-UCL-associated current.

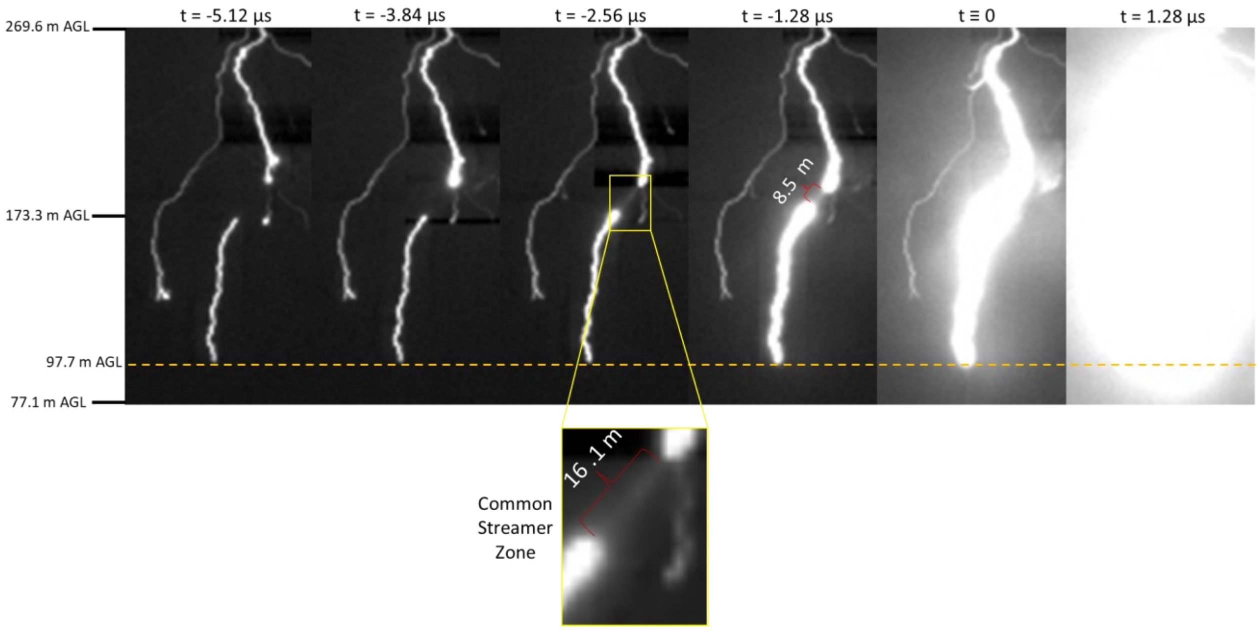

Figure 1. Six consecutive video camera frames recorded for stroke 060622. Each frame has a 740 ns exposure time and is followed by a 540 ns dead time.

3.2 – STROKE 061822

Figure 4 shows five consecutive video camera frames recorded for stroke 061822. The frame rate and FOV of the camera were identical to those for stroke 060622. In the rightmost frame we observe that the UCL and DL have attached to each other, and the return stroke is well underway, as indicated by the large enhancement in the brightness of the frame. We have labelled this frame as t ≡ 0. The CSZ was first observed three frames prior (t = -3.84 μs) to the attachment frame and had a length 11.8 m at that time. We show the zoomed-in view of the CSZ in the box below the frame. After the CSZ was formed, the UCL and DL propagated within the CSZ and in the frame (t = -1.28 μs) immediately preceding the attachment frame, the gap between the UCL and DL was just 4.3 m. Based on the smaller UCL-to-DL distance in the t = -1.28 μs frame (in this stroke compared to that in stroke 060622) and the brightness of the attachment frame (which is significantly enhanced compared to the t ≡ 0 frame of stroke 060622), we expect that the attachment of the UCL and DL in this stroke occurred toward the end of the t = -1.28 μs frame or during the dead time between this frame and the attachment frame (t ≡ 0).

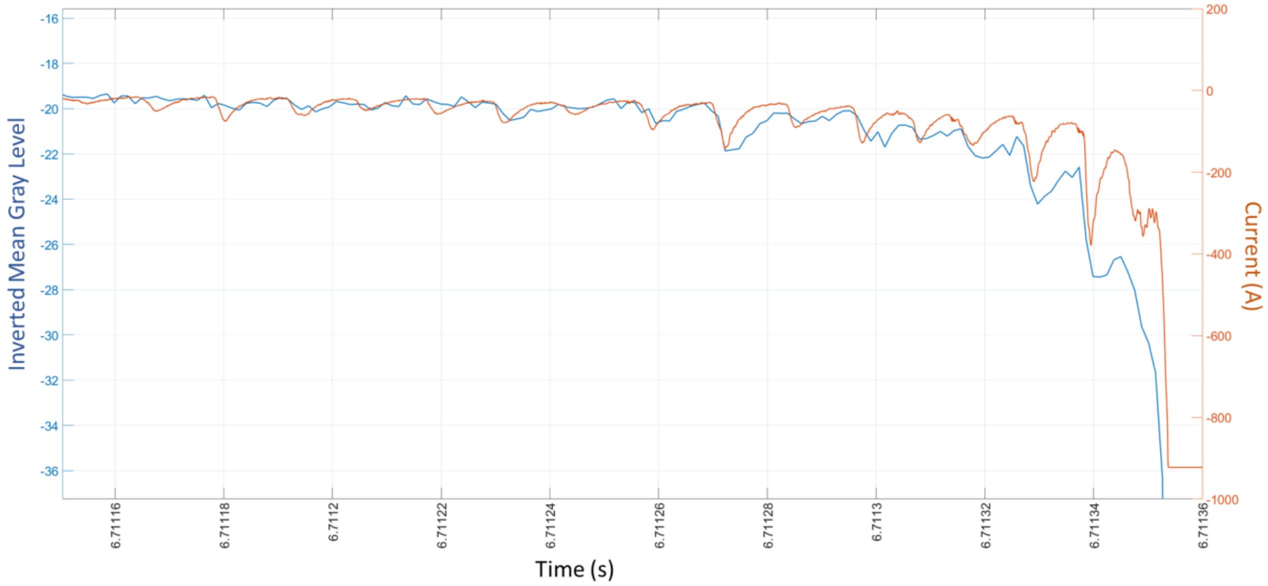

Figure 2. Time-alignment of the rising edges of luminosity and current pulses associated with the UCL in stroke 060622.

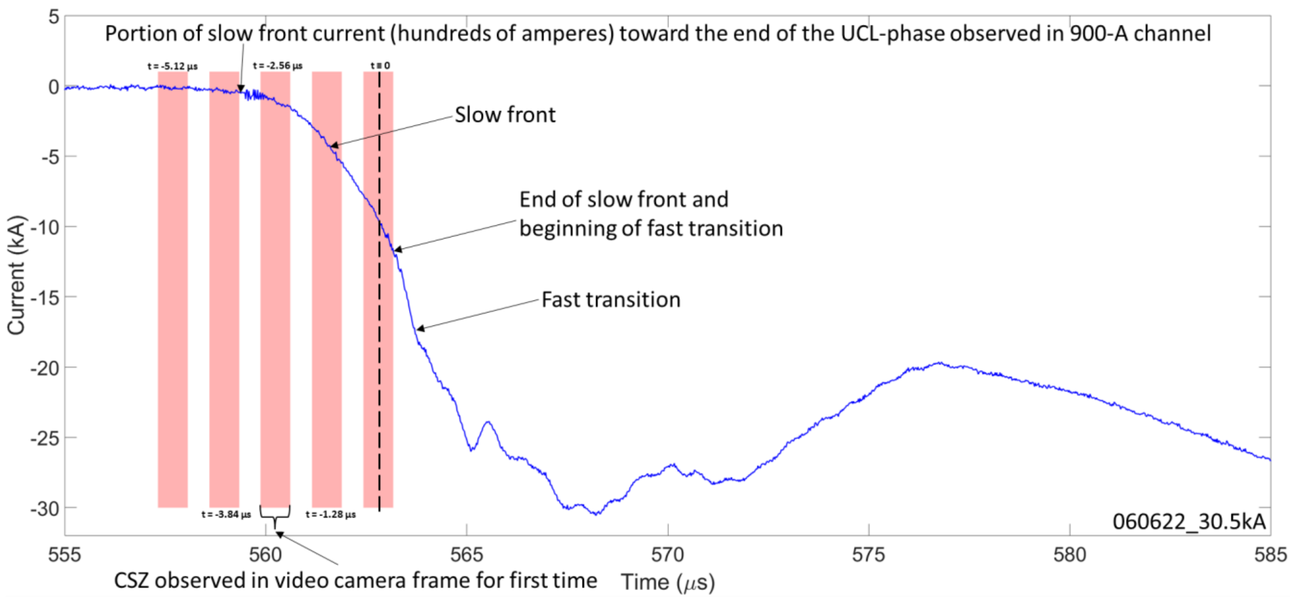

Figure 3. Overlay of the video-camera frame exposure times (indicated by pink rectangles) on top of the current waveform shown on a 30-μs time window measured by our 350-kA channel for stroke 060622.

Using the luminosity-current time-alignment (same procedure as for stroke 060622), in Figure 5 we overlaid the exposure times of our video camera frames (indicated by pink rectangles) on top of the current waveform (shown on a 32-μs time window) measured by our 350-kA channel. The corresponding times for the video camera frames are indicated above and below each rectangle. The black vertical dashed line indicates the mid-point of the exposure time of the attachment frame (t ≡ 0). For this stroke, this frame occurred in the middle of the fast transition. The alignment of the attachment frame with the middle of the fast transition instead of the end of the slow front/beginning of the fast transition is likely due to this frame being captured as the return stroke is well underway. As stated earlier, for this stroke we expect that the attachment of the UCL and DL occurred toward the end of the t = -1.28 μs frame or during the dead time between this frame and the attachment frame (t ≡ 0). Similar to stroke 060622, we observe in this case as well that the frame (t = -3.84 μs) in which the CSZ is observed for the first time aligns with the portion of the slow front waveform where the current increases rapidly from the early-UCL-associated current.

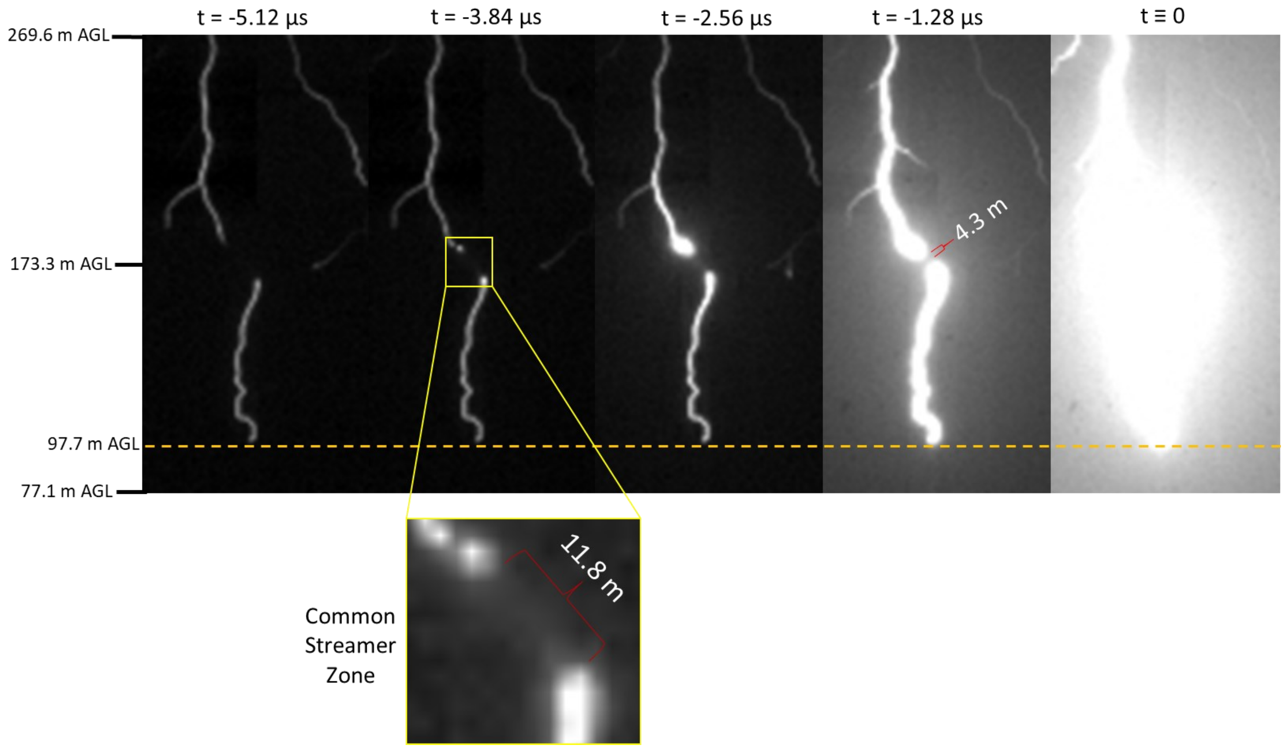

Figure 4. Five consecutive video camera frames recorded for stroke 061822. Each frame has a 740 ns exposure time and is followed by a 540 ns dead time.

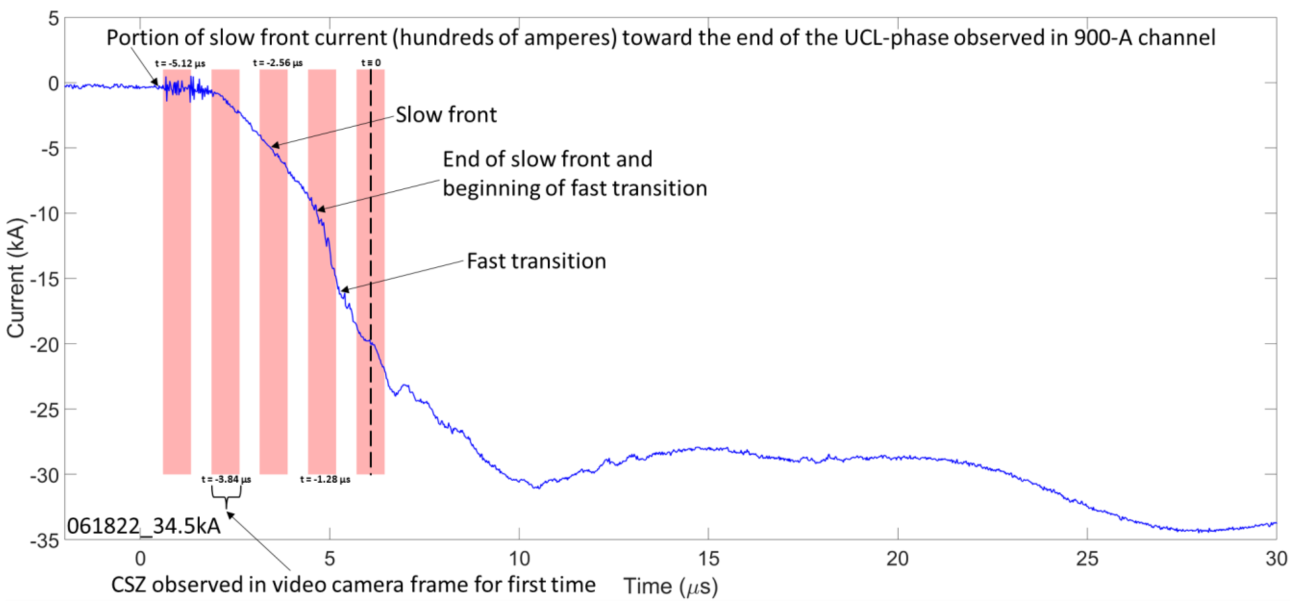

Figure 5. Overlay of the video-camera frame exposure times (indicated by pink rectangles) on top of the current waveform shown on a 32-μs time window measured by our 350-kA channel for stroke 061822.

4 – SUMMARY OF RESULTS

We examined time-correlated ultra-high-speed video camera records and channel-base current waveforms of two negative cloud-to-ground strokes that attached to the IAT in June 2022. The measured return stroke peak currents were -30.5 kA and -34.5 kA. The attachment points between the upward and downward leaders for the two strokes were 78 and 72 m above our Franklin rod (175.7 and 169.7 m AGL), respectively.

Our observations confirm that:

- The slow front in current begins during (toward the end of) the UCL phase of a stroke and a rapid increase in the slow-front current occurs associated with the formation of the CSZ.

- The attachment process is completed when the UCL and DL propagate within the CSZ and merge with each other, marking the onset of the fast transition in the current waveform.
- Thus the “return stroke proper” starts with the fast transition in current and is preceded by the UCL and CSZ phases of the stroke.

5 – REFERENCES

[1] Saba, M. M. F., da Silva, D. R. R., Pantuso, J. G., & da Silva, C. L., 2022. Close view of the lightning attachment process unveils the streamer zone fine structure. Geophysical Research Letters, 49, e2022GL101482. https://doi.org/10.1029/2022GL101482.

[2] Plaisir, M. N., Nag, A., Cummins, K. L., Biagi, C. J., Goldberg, D. J., Khounate, H., Imam, A.Y., Brown, R. G., and Rassoul, H. K. 2022. Measurements of current, magnetic field, and video on a sub-microsecond-scale at the time of downward cloud-to-ground lightning attachment, 2022 AGU Fall Meeting, Abstract AE35A-62.

[3] Jiang, R., Srivastava, A., Qie, X., Yuan, S., Zhang, H., Sun, Z., et al. (2021). Fine structure of the breakthrough phase of the attachment process in a natural lightning flash. Geophysical Research Letters, 48, e2020GL091608. https://doi.org/10.1029/2020GL091608.

[4] Qi, Q., Lyu, W., Ma, Y., Wu, B., Chen, L., Jiang, R., et al., 2019. High-speed video observations of natural lightning attachment process with framing rates up to half a million frames per second. Geophysical Research Letters, 46, 12,580–12,587. https://doi.org/10.1029/2019GL085072.

[5] Tran, M. D., & Rakov, V. A., 2017. A study of the ground-attachment process in natural lightning with emphasis on its breakthrough phase. Scientific Reports, 7(1), 1–13. https://doi.org/10.1038/s41598-017-14842-7.

[6] Khounate, H., Nag, A., Imam, A. Y., and Rassoul, H. K., 2021. The lightning attachment process in a negative cloud-to-ground stroke observed on a sub-microsecond timescale. 2021 AGU Fall Meeting, Abstract AE23A-01.

[7] Nag, A., Cummins, K. L., Plaisir, M. N., Wilson, J. G., Crawford, D. E., Brown, R. G., et al., 2021. Inferences on upward leader characteristics from measured currents. Atmospheric Research, 251 (December 2020). https://doi.org/10.1016/j.atmosres.2020.105420.

Main author
Name: Mathieu N. Plaisir
Address: 150 W University Blvd., Melbourne, FL 32901
E-mail: mplaisir2013@my.fit.edu